Spurious Numerical Oscillations in Numerical Simulation of Supersonic Flows Using Shock Capturing Schemes

Theodore K. Lee*and Xiaolin Zhong†
University of California, Los Angeles, California 90095

Abstract

The numerical simulation of transitional and turbulent processes in hypersonic boundary layers often involves a physical process of a shock-disturbance wave interaction in complex two-dimensional and three-dimensional flow fields. For such simulations, it is required that there be a high order of accuracy in capturing both the shock and the small disturbances. The purpose of this paper is to evaluate the viability of using high order shock capturing schemes to track small disturbances in a multi-dimensional steady hypersonic flow. The numerical methods that are to be studied are the Total Variation Diminishing (TVD) scheme, and Essentially Non-Oscillatory (ENO) scheme. This paper shows that the presence of numerical oscillations in the flow field solution may drastically hinder any attempt at tracking the propagation of any physical disturbances. It has been found that the numerical oscillations that exist for shock capturing methods may be significant enough to pollute a flow field containing small physical disturbances. The effects of the refinement of the grid do not reduce the oscillations, but rather they decrease the wavelength of the oscillations. It is shown that by aligning the shock with the grid, the amplitude of these spurious oscillations may be greatly reduced.

Introduction

In computing steady state hypersonic flow fields, the goal of an accurate solution is obtained by any number of high order shock capturing schemes. The simulation of transitional and turbulent processes in hypersonic boundary layers, however, will need to involve the accurate capture of the interactions between freestream waves and the bow shock. For such an investigation, both the freestream and post-shock regions must be contained within the computational domain. Shock fitting methods are used extensively in supersonic and hypersonic flow fields, however they are limited by the fact that they are unable to contain any discontinuities. It is due to this constraint that the shock capturing schemes are chosen as the numerical methods with which to simulate any complex interaction between the shock and freestream waves. Shock capturing numerical schemes such as the ENO and TVD methods have been used extensively in flows involving shocks, and have been proven to be very effective when used to solve for the general aerodynamic properties of a flow. To accurately simulate a hypersonic flow with small disturbance waves, however, the shock capturing method must generate spurious oscillations which are negligible in comparison to the physical disturbance waves. The presence of large spurious oscillations in the steady state solution will pollute the flow field, making it extremely difficult to track small disturbance waves.

An important part of this study has been to objectively examine the application of a number of popular numerical methods in the solution of hyperbolic conservation laws. There are many similar studies involving one dimensional conservation laws, however the extension to two or three dimensions is nowhere near as extensive. The presence of post-shock oscillations has been recently studied by Arora and Roe [1], Jin and Liu [2], as well as Lin [3]. Lin [3] found that for a two dimensional slowly moving shock, oscillations would appear in the post-shock region, even though previous studies with a one dimensional case produced no oscillations at all. As a cure for these unwanted oscillations, Lin suggests the use of artificial dissipation, though he admits that the amount needs to be adjusted on a case by case basis. He also points out that this behavior can be classified as non-monotone. Jin and Liu [2] also studied the post-shock oscillations found for a slowly moving shock. They note that because all shock capturing methods use some degree of artificial viscosity, a smeared shock profile will introduce a spike in the momentum at the discontinuity location. This spike, coupled with the conservation of momentum, will generate spurious oscillations. They noted that a higher order of accuracy actually accentuates the problem. With the use of scalarly monotone schemes such as TVD and ENO with non-linear systems, they expect to find that non-monotone behavior exists. Arora and Roe [1] say that the reason for these post-shock oscillations is due to the method in which the concept of monotonicity is extended from scalar conservation laws to systems. Methods such as TVD and ENO that are monotone for scalar cases, fail for systems because they are no longer mono-

*Graduate Student, theodore@seas.ucla.edu, Student Member AIAA

†Associate Professor, Mechanical and Aerospace Engineering Department, xiaolin@seas.ucla.edu, Member AIAA

tone, even with monotone initial data. Their belief is that the presence of unwanted oscillations is inevitable for shock capturing methods, and suggest a number of ways in which this problem can be alleviated. As can be seen, the study of freestream disturbances interacting with a shock over a blunt body cannot be very successful if there is already a significant amount of non-physical oscillation behind the shock. The transmission and generation of disturbances by a freestream wave would be combined with numerical oscillations that exist already, thereby polluting the solution.

For the interaction of small freestream waves with a shock, Kovasney [4] showed that weak disturbance waves in compressible flow can be decomposed into three independent modes. These modes are the acoustic, entropy and vorticity modes. The interaction of any of these three modes with a shock will generate all three behind the shock. This shock-disturbance wave interaction is shown in Figure 1. Further linearized analyses have been done by Ribner [5], Chang [6] [7], and McKenzie and Westphal [8]. These analyses also show that all three modes are generated behind the shock, irrespective of the freestream wave.

There have been many studies that have been performed for a one-dimensional shock-disturbance interaction. One form is the interaction between a shock with turbulence. Lee et. al. [9] investigated the interaction of isotropic turbulence with a weak shock wave. They found that the turbulence is enhanced during the interaction, and that turbulent energy is amplified. Mahesh et. al [10] studied the interaction between a shock wave and a turbulent field of vorticity and entropy fluctuations. They found that the turbulent kinetic energy can be either amplified or suppressed depending on the correlation between the vorticity and entropy disturbances. There are many other numerical studies on shock-turbulence interaction [11] [12] [13] [14] [15].

The purpose of this research is to investigate the interaction of freestream waves that interact with a bow shock of a blunt body. The numerical method must accurately predict the result of an interaction between a freestream wave with the bow shock, and then accurately track the generated disturbances behind the shock as well. Therefore, before such a study is begun, we must be sure that the small disturbance waves that are being tracked, are indeed being created by the interaction between the shock and the freestream waves, and not spuriously by the numerical method itself. The initial test case is a supersonic, inviscid, ideal gas flow over a circular cylinder. This is a well known flow geometry, and is a relatively simple multi dimensional flow field. The results of the ENO and TVD methods are analyzed and compared to each other.

The effect of grid resolution is first investigated. It is known that the mean flow values that are found using both the ENO and TVD methods will become more accurate as the grid is refined. The effect on the generation of spurious oscillations, however, is not as clear. It is found that the grid resolution affects the wavelength of the spurious oscillation, but has no effect on the amplitude. When the grid resolution is increased, the wavelength of the oscillations decreases. These spurious oscillations, however, were also found to be quite large, and would significantly hinder any attempt at tracking small disturbance waves through the region behind the shock.

The results showed that in certain regions of the flow, there appeared to be no generation of oscillations. It was concluded that this was due to the shock being very well aligned with the grid. A method involving the use of a modified grid, so that the shock that has been captured is aligned closely with a grid line, was used to attempt to reduce the amount of oscillations being generated. Arora and Roe [1] noted that multi-dimensional flows involving shock capturing methods will inevitably result in unwanted spurious oscillations. The effect of aligning the shock with the grid, therefore, is to produce a geometry that is as close to one-dimensional as possible in the computational domain. This method is attempted because it has been shown that there are no spurious oscillations for a one-dimensional test case. The method of aligning the grid with the shock has recently been used by Carpenter and Casper [16]. However, their focus was on the order with which a numerical method captures the shock, rather than the oscillations that are generated behind it. The results show that the effect of aligning the shock with the grid will greatly reduce the amplitude of the numerical oscillations.

GOVERNING EQUATIONS

The governing equations for simulating fluid flows consist of the Navier-Stokes equations. For an inviscid flow, the Navier-Stokes equations would simplify into the Euler Equations.

The two-dimensional Euler equations are as follows:

$$\frac{\partial U}{\partial t} + \frac{\partial F}{\partial x} + \frac{\partial G}{\partial y} = 0 \tag{1}$$

where,

$$U = \begin{bmatrix} \rho \\ \rho u \\ \rho v \\ E \end{bmatrix}, F = \begin{bmatrix} \rho u \\ \rho u^2 + P \\ \rho uv \\ uE \end{bmatrix}, G = \begin{bmatrix} \rho v \\ \rho uv \\ \rho v^2 + P \\ vE \end{bmatrix}.$$

P is the pressure, ρ is the density, u and v are the horizontal and vertical velocities, and E is the energy. The equation of state is :

$$P = \rho RT \tag{2}$$

where R is the universal gas constant and T is the temperature. The freestream was comprised of diatomic nitrogen, therefore the specific heat ratio γ was set to 1.4.

Numerical Methods

The shock capturing methods that have been studied are the Total Variation Diminishing (TVD) scheme [17], and the Essentially Non-Oscillatory (ENO) scheme [18]. We also studied the Weighted Essentially Non-Oscillatory (WENO) scheme [19], and a Monotone Upstream Scheme for Conservation Laws (MUSCL) [20]. This paper, however, will focus on only the ENO and TVD schemes. The WENO scheme was found to be qualitatively similar to the ENO scheme, and the MUSCL scheme was found to be qualitatively similar to the TVD scheme. We also chose to concentrate on the ENO and TVD schemes due to the fact that they seem to be among the more popular shock capturing methods being used today.

All shock capturing schemes will possess unwanted spurious numerical oscillations in a multi-dimensional simulation. It would, therefore, be extremely difficult to find suitable shock capturing solution with which to use as a comparison for the ENO and TVD solutions. As a result, we have chosen to use a high order shock fitting numerical scheme to use as an exact solution, since the shock fitting solutions contain no spurious oscillations.

Essentially Non-Oscillatory (ENO)

The ENO schemes of Harten et. al. [18] were developed by ensuring the calculated flux was always based on the smoothest stencil. This method of adaptive stencils ensures that the solution will maintain a high order of accuracy. This is especially important in regions of discontinuity, such as shocks. Therefore, the use of the ENO schemes in flows involving shocks has become highly popular. Previous studies of flow fields involving shocks using the ENO schemes include Chiu and Zhong's [21] study of a transient hypersonic flow, as well as Mahesh et. al. [22], who studied the interaction of a shock wave with a turbulent shear flow.

The ENO scheme that was chosen to be used in this study is the finite-difference version of Shu and Osher [23]. This scheme was chosen because of its simple implementation into multi-dimensional problems. The finite-difference schemes also avoid the costly cell reconstruction procedure of the finite-volume ENO scheme, thereby improving the computational efficiency.

The accuracy of the ENO scheme is adjustable, due to the specification of the stencil size. In this study, the ENO scheme was set to have third-order accuracy. For the third-order ENO scheme, the approximation of the flux terms are based on one of three possible stencils. These three stencils are :

$$(i-2, i-1, i),$$

$$(i-1, i, i+1),$$

$$(i, i+1, i+2).$$

The ENO scheme selects which stencil to use to approximate the flux based on the smoothness of the stencils. The smoothest stencil will be the one that is used. This ensures that the numerical approximations will always avoid discontinuities and the large gradients associated with them.

Total Variation Diminishing (TVD)

The use of TVD schemes in the solution of hyperbolic conservation laws is widespread. It has been a popular method ever since the original concept was introduced by Harten [17]. While many variations on the TVD method have been developed, the basis of all of them remains the same. Previous studies involving the TVD schemes include Yee and Warming's [24] study of a divergent nozzle and a two-dimensional shock reflection problem. The TVD scheme has also been used by Peroomian et. al. [25] for the study of a confined shear layer.

The TVD method is based on the idea of choosing the smallest flux value if all the other approximations to the flux are of the same sign, and to choose a flux value of zero, if the approximations of the flux are of different sign. This ensures that there will be no new local extrema created, and that the TVD schemes are monotonicity preserving.

Because there have been so many variations on the TVD method, a simple one that was used by Furumoto et. al. [26] was chosen. The approximation to the flux $f_{i+1/2}$ is as follows :

$$f_{i+1/2} = F_{i+1} - \frac{1}{2} minmod[\Delta_{i+1}, \Delta_i] \qquad (3)$$

where,

$$\Delta_i = F_{i+1} - F_i. \qquad (4)$$

The minmod function is responsible for choosing the smallest stencil if both values of Δ are of the same sign, or zero if the two values are of opposite signs. It can be formulated as :

$$minmod(a, b) = \frac{1}{2}[sgn(a) + sgn(b)]min(|a|, |b|)$$

In considering computational efficiency, the TVD scheme involves much less computations than the ENO scheme. This translates into a faster, more efficient program. When considering accuracy though, the TVD scheme reduces to only first order accuracy at discontinuities, whereas the ENO scheme is able to maintain third order accuracy at discontinuities. The accuracy at the discontinuities is a concern because the accuracy with which the numerical method captures the interaction between the shock and a disturbance wave is very important.

Shock Fitting

The shock fitting solutions is only used as an exact solution with which to compare the ENO and TVD

solutions to. The errors that are calculated for the ENO and TVD methods are in relation to the shock fitting solution. The difference between shock capturing schemes and shock fitting schemes is that the shock fitting scheme uses the shock as its outer boundary, whereas the shock capturing schemes capture the shock. Because the shock fitting schemes do not capture the shock, there are no spurious oscillations generated behind the shock. This provides a solution free of oscillations with which the ENO and TVD schemes can be compared to.

The shock fitting schemes have a disadvantage in that they cannot solve for flow fields which contain complex shock-wave or shock-shock interactions. The shock capturing schemes, on the other hand, are able to simulate these complex shock interactions.

We will not go into the details of the shock fitting algorithm here. For reference, however, we used the shock fitting algorithm previously used by Zhong [27] [28] to simulate a hypersonic flow over a blunt body.

Results

The test case that has been used is the Mach 4 two-dimensional cylinder numerical test case of Kopriva [29]. He uses a spectral code in order to calculate the steady state solution. The spectral code has a high-order of accuracy, and it was deemed a better test case than a lower order numerical scheme, or experimental case. This type of supersonic flow was also chosen because it is a rather simple, and commonly used two-dimensional geometry. The published results of Mach, pressure and entropy contours allowed for a comparison to the computed solutions to ensure that the ENO and TVD methods were calculating the correct results.

Steady State Solution

The initial solutions for both the ENO and TVD schemes were computed using the exact same computational grid. This grid has a resolution of 102×120 and is shown in Figure 2. By using the same grid, the TVD and ENO schemes can be easily compared to each other, with any differing results to be independent of the grid. This grid resolution was chosen because it would present an accurate solution without severely restricting computational time.

The mean flow variables of this supersonic flow are shown in Figures 3, 4, 5, and 6. These are the density, temperature, pressure and entropy contours respectively. As can be seen, there are no highly visible signs of spurious oscillations in the solution. The temperature contours contain a very small rippling effect behind the upper shock. This rippling, however, does not seem to have a large effect on the temperature results. There is no doubt that the ENO and TVD schemes are very accurate and highly reliable when it comes to computing mean flow variables.

The problem involving the ENO and TVD schemes is when the interest lies in simulating the interaction between a disturbance wave with the shock, or other such small scale phenomenon. Such simulations require the shock capturing schemes to be able to track small disturbance waves as they travel through the entire flow field. If the spurious oscillations that are generated by the numerical scheme are negligible in comparison to these disturbance waves, then they can be accurately tracked. However, if the disturbance waves are of the same order, or negligible in comparison to the spurious oscillations, then it would be extremely difficult to track them through the flow field.

While the mean flow values do not show the presence of any spurious oscillations, an analysis of the vorticity contours clearly shows oscillatory behavior. These oscillations may be easily seen in Figure 7. It shows that the magnitude of these waves may dramatically hinder any attempt at capturing any sort of small scale phenomena. The contours for the ENO and TVD schemes are not similar in some regions of the flow. This is due to the high amount of numerical dissipation inherent in the TVD scheme, which acts to smooth out the solution much more than the ENO scheme. The vorticity contours, therefore, seem to be much smoother for the TVD scheme than for the ENO scheme. The vorticity contours for the WENO and MUSCL scheme are shown in Figure 8. Clearly, they exhibit the same qualitative behavior as the ENO and TVD schemes respectively.

The location of these spurious oscillations shows the effect that the numerical grid has on the generation of them. There appears to be common regions of the flow that are free of oscillations, while other areas possess large oscillations. In the region behind the shock near the stagnation line, there doesn't appear to be any spurious oscillations being generated. It is only as the shock becomes more oblique, that these oscillations begin to appear, and grow in magnitude. This is due to the fact that at the stagnation line region, the shock is very well aligned with a grid line. If the shock is aligned with a grid line, it will be sharply captured, and as a result, generate very little or no spurious oscillations. As the shock becomes more oblique, it also diverges more from the grid lines, thereby generating larger oscillations. It has been previously reported that these two numerical methods show no oscillations for a one dimensional problem. This is due to the fact that in a one-dimensional problem, the shock will always be aligned perfectly with the grid. In the oblique shock region, however, the shock is not aligned with the grid. This clearly results in a two dimensional problem and the post-shock oscillations that are produced from it.

To determine the magnitude and extent that these numerical methods are producing oscillations, a shock fitting solution is used for comparison. The pressure and vorticity contours of the shock fitting scheme are shown in Figure 9. The pressure contours are nearly

identical to the ones shown in Figure 5 for the ENO and TVD solutions. The vorticity contours, however, are completely free of any evidence of spurious oscillations.

Grid Refinement

With computational power increasing every year, computationally simulating transitional and turbulent processes have become more focused on capturing small scale structures. With more powerful computers, the grid resolution of many flow fields can be increased with the reasoning that a finer grid will be better able to capture finer structures. The effect of grid resolution on the generation of spurious oscillations in flows containing discontinuities has not clearly been studied. We have found that by using the shock capturing methods, the generation of spurious oscillations may actually increase with finer grid resolution, thereby possibly concealing any small scale structures that may be present in the flow.

It has been shown that a discontinuity that is not aligned well with the grid has a large effect on the generation of unwanted oscillations. The resolution of the grid may also have an effect on the magnitude and amount of oscillations present in the solution. Our results show that the use of a finer grid resolution may, in fact, have a negative effect of generating more oscillations. This would make it extremely difficult to track small scale disturbances through a discontinuity. A high grid resolution would be required to capture a small disturbance wave, yet it would also result in more spurious oscillations.

The use of three numerical grids of different size allows for a study on the effects of the grid resolution on the generation of numerical oscillations. The original grid with which the supersonic cylinder flow case was computed with has a grid resolution of 102×120. Two additional grids have been used and solved for this flow using both the ENO and TVD schemes. The first grid is a coarse grid with a resolution of 60×60. The second grid is a fine grid with a resolution of 186×240.

We have chosen to take line distributions through 2 different sections of the flow field. The first line distribution is behind the shock as shown in Figure 10. The second line distribution is a line that is normal to the wall, as shown in Figure 11. By comparing the locations of both the line distributions with the vorticity contours of Figure 7, it can be seen that both distributions pass through areas with a low amount of oscillations as well as a high amount of oscillations.

The grid resolution, obviously has a direct effect on the accuracy of the solution. To show that the ENO and TVD become more accurate for mean flow values when the grid resolution is increased, the pressure behind the shock is shown in Figures 12 and 13 respectively. The pressure distributions normal to the wall are shown in Figures 14 and 15 for the ENO and TVD schemes respectively. We assume that the shock fitting solution is the most accurate. It can be seen that, as expected, the pressure approaches the shock fitting solution as the grid is refined. For mean flow values, the finer the grid, the more accurate the solution will be. The use of shock capturing methods for the computation of mean flow values in a flow field containing discontinuities is extremely good.

For small scale structures, however, the correlation between grid resolution and accuracy is not as well known. Previously, the vorticity contours were shown to be a good indicator of the presence of spurious oscillations. The vorticity contours for the coarse grid are now shown in Figure 16. The vorticity contours for the fine grid are shown in Figure 17. While there does not seem to be any drastic differences between the 3 different sized grids for the TVD scheme, the ENO scheme shows some large differences in the amount of spurious oscillations. The TVD scheme does not show a large difference, again, due to the large amounts of numerical dissipation it possesses. The ENO scheme, however, seems to show that the oscillations become worse as the grid is refined. This result is in contrast to the mean flow values, which become more accurate.

The vorticity line distribution behind the shock is shown in Figures 18 and 19 for the ENO and TVD methods respectively. It can be seen that the spurious oscillations become worse as the grid is refined. The line distribution begins close to the stagnation line region, therefore containing no oscillatory behavior. As the line proceeds into the oblique shock region, the oscillations begin to develop. The ENO solution in Figure 18 especially, shows that the amplitude of the oscillations is approximately the same with increasing grid resolution. It does, however, show that the wavelength decreases with grid resolution. The wavelength is linked to the grid resolution by the distance between neighboring grid lines. The grid lines become closer as the grid is refined. The wavelength decreases because of the decreasing distance between the grid lines. The TVD results show that the amount of numerical dissipation in this method greatly reduces the oscillations when compared to the ENO results. However, the fine grid result still produces more oscillations than the coarse grid result. By reducing to first order accuracy at the shock, the production of spurious oscillations is much less than those produced by the ENO method. The reduction to first order at discontinuities, however, results in a loss of accuracy in the mean flow values.

The l_1 and l_2 errors for vorticity are shown in Table 1 for the ENO scheme, and in Table 2 for the TVD scheme.

The ENO results show no significant changes in the relative error, for either the l_1 or l_2 error. This is expected since the amplitude of the oscillations is approximately equal in all three grid cases. The effect that the grid has on the oscillation wavelength will not appear in

Table 1: Vorticity Relative Error Behind the Shock for the ENO scheme.

Grid	l_1 Error	l_2 Error
60×60	0.044467	0.003787
102×120	0.036943	0.003437
186×240	0.039323	0.003558

Table 2: **Vorticity Relative Error Behind the Shock for the TVD scheme.**

Grid	l_1 Error	l_2 Error
60×60	0.026105	0.002111
102×120	0.017729	0.001538
186×240	0.012558	0.001108

this error analysis. The TVD results show that the results seem to improve with finer grid resolution. This is because even though the finer grid resolution produces a larger amplitude of spurious oscillations, the coarse grid results were not as close to the shock fitting solution. Therefore, even though the fine grid relative error is less, the amount of oscillation is larger.

The vorticity line distributions for the wall normal line are shown in Figures 20 and 21 for the ENO and TVD schemes respectively. These results support our conclusion involving the vorticity line distributions behind the shock. Again for the ENO case, the oscillations possess approximately the same amplitude while decreasing in wavelength behind the shock for higher grid resolution. The TVD case shows the effects of its numerical dissipation. The errors are tabulated in Tables 3 and 4 for the ENO and TVD methods.

Table 3: **Vorticity Relative Error Normal to the Wall for the ENO scheme.**

Grid	l_1 Error	l_2 Error
60×60	0.043290	0.003906
102×120	0.034071	0.003798
186×240	0.042506	0.004470

Similar to the results for relative error behind the shock, the error results for the ENO method stay approximately the same, while the TVD results improve with increasing grid resolution. Again, the wavelength of the ENO results will have no effect on the relative error, and the TVD method's numerical dissipation manages to damp out most of the spurious oscillations. Similar to mean flow values, the TVD method shows an improvement in accuracy with increasing grid resolution.

Table 4: Vorticity Relative Error Normal to the Wall for the TVD scheme.

Grid	l_1 Error	l_2 Error
60×60	0.065359	0.007397
102×120	0.020568	0.002238
186×240	0.013617	0.001336

Grid Alignment

Previously, it has been found that the region near the stagnation line contains very little numerical oscillations, whereas the region behind the oblique shock contains a high amount of oscillations. It was concluded that this was due to the fact that the grid lines and shock are very well aligned near the stagnation region, but not aligned at all as the shock became more oblique. As a possible remedy to the problem of spurious oscillations, it was desired to see how much of an effect adjusting the numerical grid to 'fit' the shock would have on reducing oscillations. The previous grid (Figure 2) was generated using a quadratic polynomial. By generating a new grid using a fourth order polynomial, this new grid can be roughly aligned with the shock location that was previously found with the quadratic polynomial grid. The new grid will not be perfectly aligned with the shock. As a result, there are still spurious oscillations being generated by the two numerical methods. The goal is to reduce the oscillations enough, so that small disturbance waves can be tracked accurately through the flow field. The new grid resolution is still 102×120, however the total size has been slightly altered to account for the alignment of the grid lines with the shock.

The vorticity contours for the ENO and TVD methods, using the grid that is aligned with the shock are shown in Figure 22. When these results are compared to Figure 7, the reduction in spurious oscillations is quite significant. Again, there is not much difference between the TVD results, due to the large amount of numerical dissipation. The ENO scheme, however, shows a significant amount of smoothing of the vorticity contour lines. These results support our conclusion that the generation of the spurious oscillations seems to be from the crossing of grid lines by discontinuities. Once a discontinuity is roughly aligned with the grid, the results contain much less oscillatory behavior. If the shock and grid were perfectly aligned, we would expect to see that the vorticity contours would closely match the shock fitting solution in Figure 9.

The vorticity distributions behind the shock are shown in Figure 23 and 24 for the ENO and TVD

schemes respectively. The ENO method shows a large reduction in the amplitude of the oscillation when used with a grid that is aligned with the shock. The wavelength, however, does not change by a noticeable amount. This supports the conclusion that the wavelength is dependent on the grid spacing. While the two different grids are not identical, they are very similar in size and grid spacing. The TVD method does not show a large improvement, but based on past results this is expected.

The relative errors for the line distributions behind the shock are shown in Tables 5 and 6 for the ENO and TVD schemes.

Table 5: **Grid Aligned Vorticity Relative Error Behind the Shock for the ENO scheme.**

Grid	l_1 Error	l_2 Error
Normal Grid	0.039154	0.003521
Grid Aligned	0.015327	0.001352

Table 6: **Grid Aligned Vorticity Relative Error Behind the Shock for the TVD scheme.**

Grid	l_1 Error	l_2 Error
Normal Grid	0.017729	0.001538
Grid Aligned	0.017182	0.001479

The ENO method shows significant improvement in both the l_1 and l_2 relative errors. The grid that is aligned with the shock manages to reduce the errors by over a factor of 2. This is due to the reduction of the amplitude of the oscillations. The TVD did not show the improvement that the ENO method did. The numerical dissipation in the TVD scheme seems to be sufficient in damping out the spurious oscillations, resulting in relative errors that are almost equal to each other.

The vorticity distributions normal to the wall are shown in Figures 25 and 26 for the ENO and TVD schemes respectively. Again, similar to the conclusions found from the results behind the shock, the ENO method generates a spurious oscillation that has a much smaller amplitude when its grid is aligned with the shock. The TVD method shows the effect of numerical damping that is expected. Tables 7 and 8 show the relative errors.

The ENO method shows the same improvement in relative errors that were found behind the shock. The reduction of the amplitude decreases the l_1 and l_2 errors by a large amount. The TVD method follows its pattern

Table 7: **Grid Aligned Vorticity Relative Error Normal to the Wall for the ENO scheme.**

Grid	l_1 Error	l_2 Error
Normal Grid	0.034071	0.003798
Grid Aligned	0.018152	0.001665

Table 8: **Grid Aligned Vorticity Relative Error Normal to the Wall for the TVD scheme.**

Grid	l_1 Error	l_2 Error
Normal Grid	0.020568	0.002238
Grid Aligned	0.022886	0.002402

of producing errors of roughly the same size, regardless of whether the grid is aligned or not.

Conclusions

The main focus of this paper was to determine the degree in which each numerical scheme provides a steady solution that is free of spurious oscillations and the effect of the grid that is used. Since the study of shock-disturbance interaction involves the tracking of small oscillations in the flow, a numerical scheme that has negligible spurious oscillations must be used. While it has been shown that the more popular methods in use today all exhibit some sort of oscillatory behavior, this behavior can be reduced significantly through an alignment of the shock with the grid.

The effect of grid resolution has been shown to decrease the wavelength, but not affect the amplitude of spurious oscillations, especially when using the ENO method. While a finer grid will produce a more accurate solution for mean flow values, it could seriously hinder any attempts at tracking small disturbances and capturing small scale structures in transitional and turbulent flows.

The production of spurious oscillations seems to stem from a discontinuity that crosses over a number of grid lines. When the grids are aligned well with the shock, the amplitude of unwanted oscillations is greatly reduced, especially in the ENO scheme. This is extremely important if we wish to track small disturbances that originate in the freestream and propagate through a shock to impact a body. If the spurious oscillations are great enough so that a small disturbance wave behind the shock becomes negligible in comparison, then the results obtained will become highly inaccurate. The wavelength, however, is unaffected by the alignment of the grid.

The ENO and TVD numerical methods are robust

and very accurate when mean flow variables are to be calculated. However, the use of these methods when small disturbance waves need to be tracked is a problem. The accurate simulation of transitional and turbulent processes in a hypersonic flow field may depend on using a shock capturing scheme which produces spurious oscillations that are negligible when compared to the disturbance waves. Even with more powerful computers, it has been shown that grid resolution may not be the solution to accurately simulating small scale structures, and small amplitude waves. The TVD method is much better than the ENO method at generating smooth solutions, but the fact that this scheme reduces to first order accuracy at discontinuities puts into question the accuracy it would have in simulating a shock-disturbance interaction.

Work is under way which includes the extension of the numerical code to handle three-dimensional geometries. The study of alternative methods to reduce spurious oscillations that appear when using the shock capturing methods is being done. Eventually the goal is to study freestream disturbances impacting on a shock over a three-dimensional body in a hypersonic flow.

Acknowledgements

This research was partially supported by the Air Force Office of Scientific Research under grant number F49620-95-1-0405 and F49620-97-1-0030 monitored by Dr. Len Sakell, and NASA Dryden Flight Research Center under Grant NCC 2-374.

References

[1] M. Arora and P. L. Roe. On postshock oscillations due to shock capturing schemes in unsteady flows. *J. Computational Physics*, 130:25–40, 1997.

[2] S. Jin and J. G. Liu. The effects pf numerical viscosities. *J. Computational Physics*, 126:373–389, 1996.

[3] H. C. Lin. Dissipation additions to flux-difference splitting. *J. Computational Physics*, 117:20–27, 1995.

[4] L. S. G. Kovasney. Turbulence in supersonic flow. *J. Aeronautical Sciences*, 20(10):657–682, 1953.

[5] H. S. Ribner. Convection of a pattern of vorticity through a shock wave. *NACA TR 1164*, 1954.

[6] C. T. Chang. On the interaction of weak disturbances and a plane shock of arbitrary strength in a perfect gas. *PhD. Thesis, John Hopkins University*, 1955.

[7] C. T. Chang. Interaction of a plane shock and oblique plane disturbances with special reference to entropy waves. *J. Aeronautical Sciences*, 24:675–682, 1957.

[8] J. F. McKenzie and K. O. Westphal. Interaction of linear waves with oblique shock waves. *Physics of Fluids*, 11(11):2350–2362, 1968.

[9] S. Lee, S. K. Lele, and P. Moin. Direct numerical simulation of isotropic turbulence interacting with a weak shock wave. *J. Fluid Mech.*, 251:533–562, 1993.

[10] K. Mahesh, S. K. Lele, and P. Moin. The influence of entropy fluctuations on the interaction of turbulence with a shock wave. *J. Fluid Mech.*, 334:353–379, 1997.

[11] K. Mahesh, S. Lee, S. K. Lele, and P. Moin. The interaction of an isotropic field of acoustic waves with a shock wave. *J. Fluid Mech.*, 300:383–407, 1995.

[12] R. Hannappel and R. Friedrich. Interaction of isotropic turbulence with a normal shock wave. *Appl. Scientific Research*, 51:507–512, 1993.

[13] S. Lee, S. K. Lele, and P. Moin. Interaction of isotropic turbulence with a strong shock wave. *AIAA 94-0311*, 1994.

[14] J. Anyiwo and D. M. Bushnell. Turbulence amplification in shock-wave boundary-layer interaction. *AIAA J.*, 20(7), 1982.

[15] T. A. Zang, M. Y. Hussaini, and D. M. Bushnell. Numerical computations of turbulence amplification in shock-wave interactions. *AIAA Journal*, 22(1):13–21, January 1984.

[16] M. H. Carpenter and J. H. Casper. The accuracy of shock capturing in two spatial dimensions. *AIAA 97-2107*, 1997.

[17] A. Harten. High resolution schemes for hyperbolic conservation laws. *J. Computational Physics*, 49:357–393, 1983.

[18] A. Harten, B. Engquist, S. Osher, and S. Chakravarthy. Uniformly high order accurate essentially non-oscillatory schemes iii. *J. Computational Physics*, 71:231–303, 1987.

[19] G. S. Jiang and C. W. Shu. Efficient implementation of weighted eno schemes. *J. Computational Physics*, 126:202–228, 1996.

[20] S. Yamamoto and H. Daiguji. Higher-order-accurate upwind schemes for solving the compressible euler and navier-stokes equations. *Computers and Fluids*, 22(2/3):259–270, 1993.

[21] C. Chiu and X. Zhong. Simulation of transient hypersonic flow using the eno schemes. *AIAA 95-0469*, 1995.

[22] K. Mahesh, P. Moin, and S. K. Lele. The interaction of a shock wave with a turbulent shear flow. *Report No. TF-69, Thermosciences Division, Department of Mechanical Engineering, Stanford University*, 1996.

[23] C. W. Shu and S. Osher. Efficient implementation of essentially non-oscillatory shock-capturing schemes. *J. Computational Physics*, 77, 1988.

[24] H. C. Yee and R. F. Warming. Implicit total variation diminishing (tvd) schemes for steady-state calculations. *J. Computational Physics*, 57:327–360, 1985.

[25] O. Peroomian, R. E. Kelly, and S. Chakravarthy. Spatial simulations of a confined supersonic shear layer at two density ratios. *AIAA 96-0783*, 1996.

[26] G. H. Furumoto, X. Zhong, and J. C. Skiba. Unsteady shock-wave reflection and interaction in viscous flows with thermal and chemical nonequilibrium. *AIAA 96-0107*, 1996.

[27] Xiaolin Zhong. Direct numerical simulation of hypersonic boundary-layer transition over blunt leading edges, part i: A new numerical method and validation. *AIAA 97-0755*, 1997.

[28] Xiaolin Zhong. Direct numerical simulation of hypersonic boundary-layer transition over blunt leading edges, part ii: Receptivity to sound. *AIAA 97-0756*, 1997.

[29] D. A. Kopriva, T. A. Zang, and M. Y. Hussaini. Spectral methods for the euler equations: The blunt body problem revisited. *AIAA Journal*, 29(9):1458–1462, 1991.

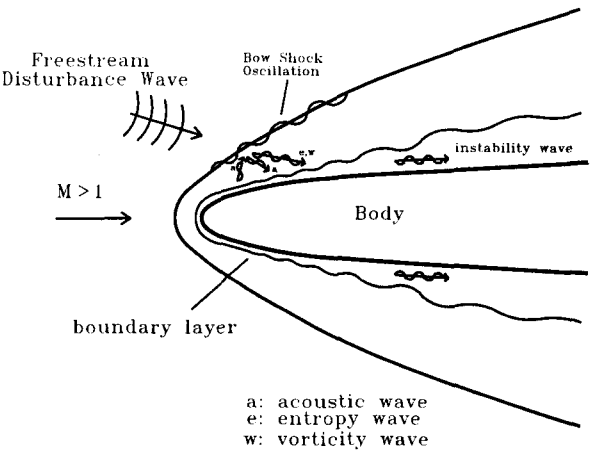

Figure 1: Freestream Disturbances Interacting with a Supersonic Blunt Body.

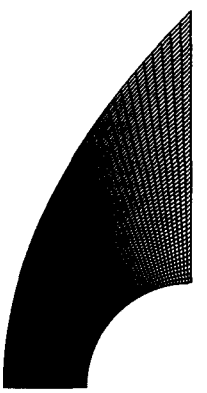

Figure 2: Numerical Grid for Mach 4 Circular Cylinder Validation Case.

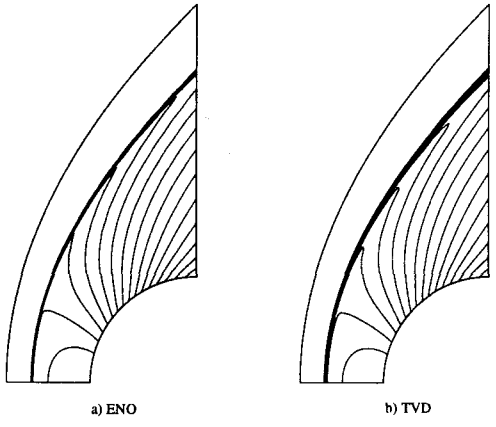

Figure 3: Density Contours for ENO and TVD Solutions.

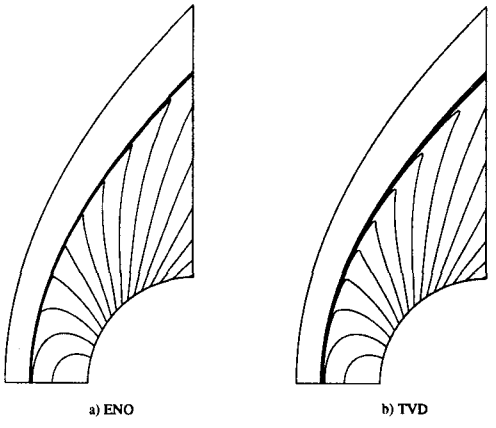

Figure 5: Pressure Contours for ENO and TVD Solutions.

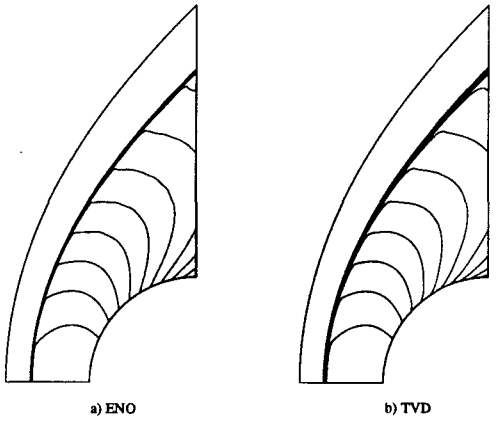

Figure 4: Temperature Contours for ENO and TVD Solutions.

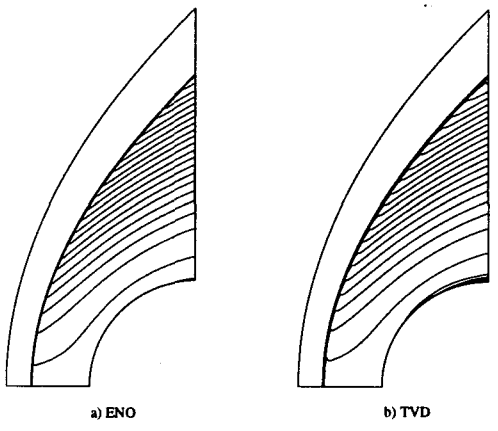

Figure 6: Entropy Contours for ENO and TVD Solutions.

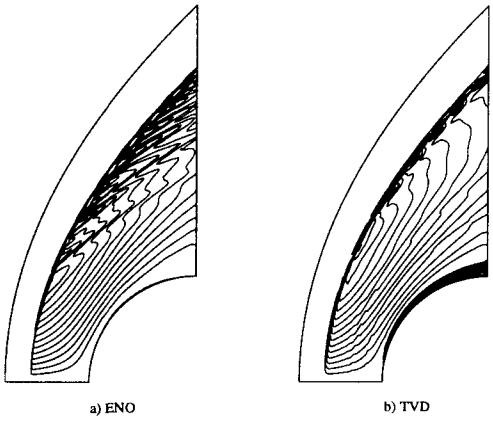

Figure 7: Vorticity Contours for ENO and TVD Solutions.

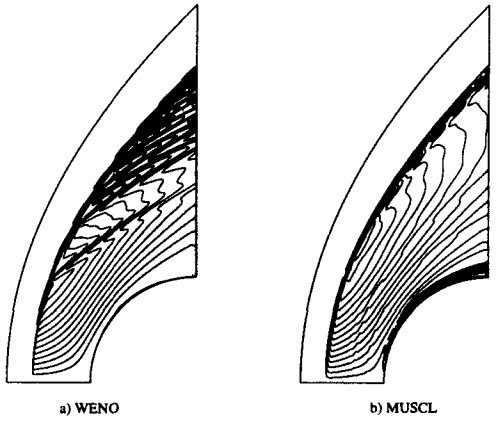

Figure 8: Vorticity Contours for WENO and MUSCL Solutions.

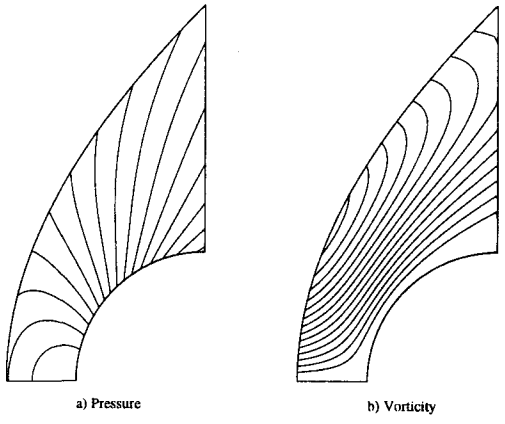

Figure 9: Pressure and Vorticity Contours for Shock Fitting Solution.

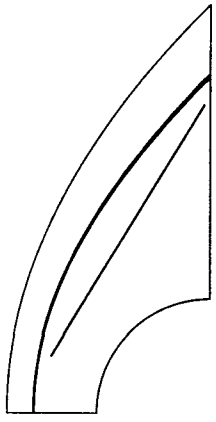

Figure 10: Line Distribution Behind the Shock.

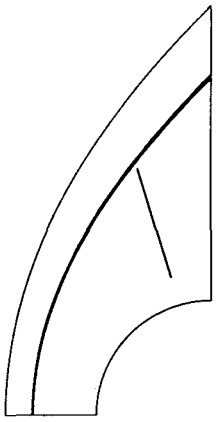

Figure 11: Line Distribution Normal to the Wall.

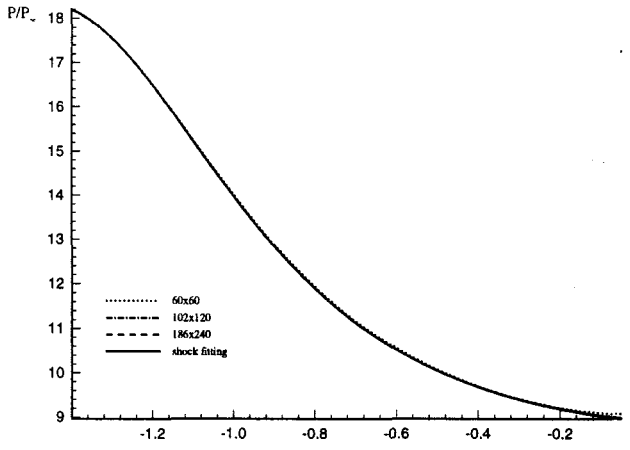

Figure 13: Pressure Distribution Behind the Shock for TVD Scheme.

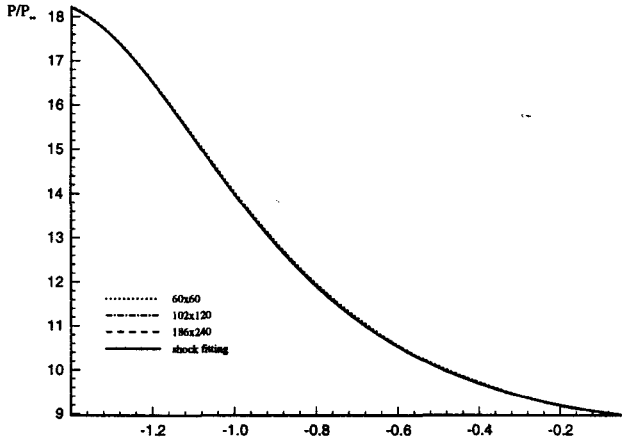

Figure 12: Pressure Distribution Behind the Shock for ENO Scheme.

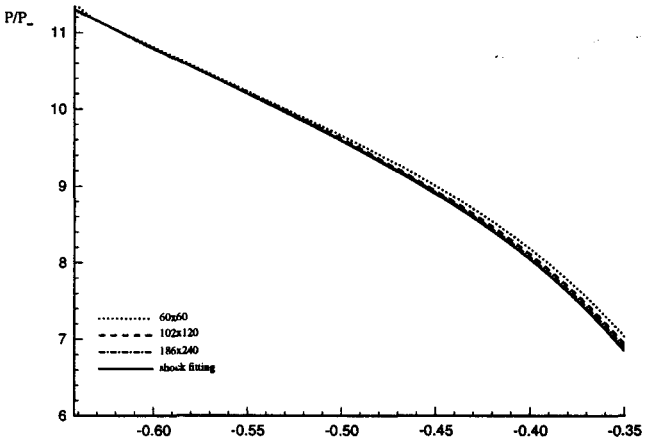

Figure 14: Pressure Distribution Normal to the Wall for ENO Scheme.

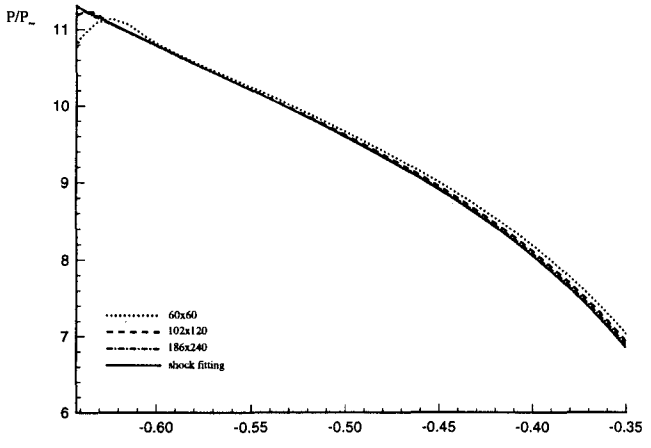

Figure 15: Pressure Distribution Normal to the Wall for TVD Scheme.

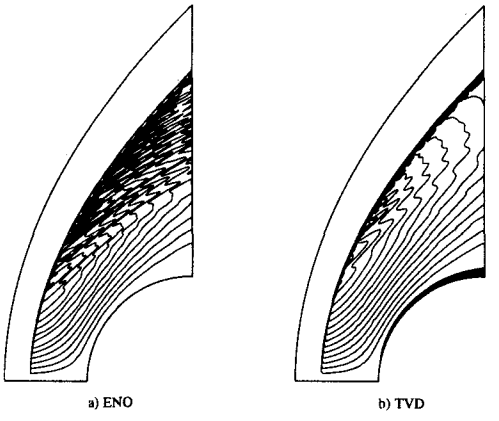

Figure 17: Vorticity Contours Using a Fine Grid for the ENO and TVD Scheme.

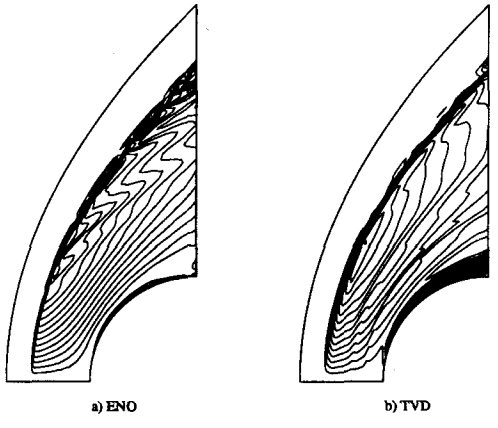

Figure 16: Vorticity Contours Using a Coarse Grid for the ENO and TVD Scheme.

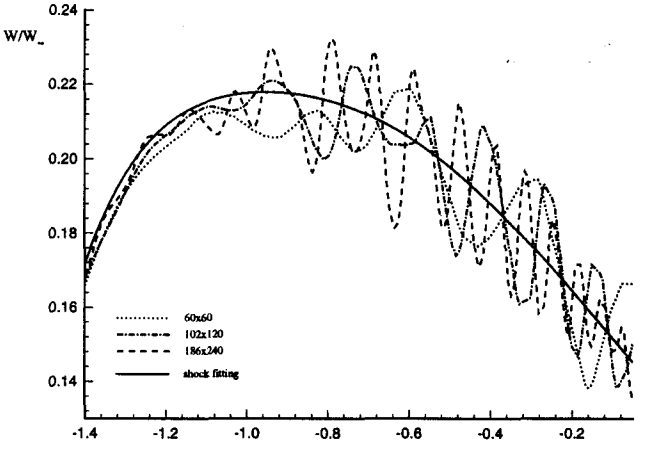

Figure 18: Vorticity Distribution Behind the Shock for ENO Scheme.

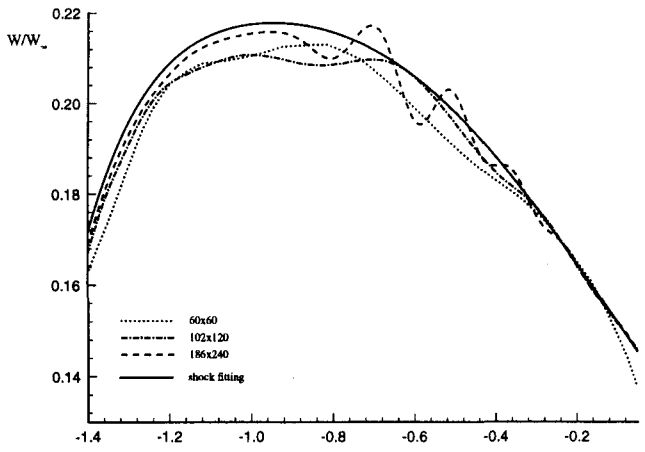

Figure 19: Vorticity Distribution Behind the Shock for TVD Scheme.

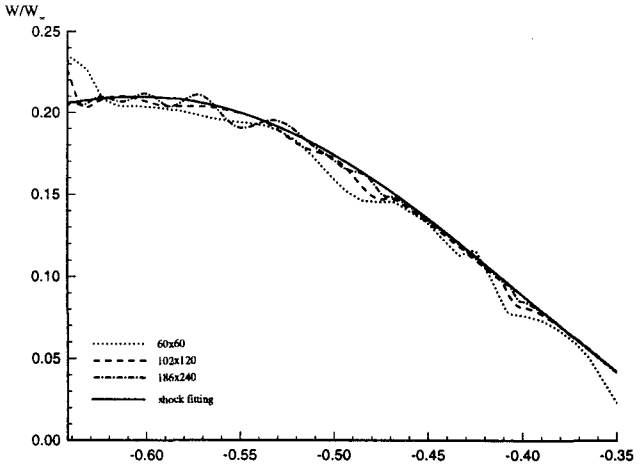

Figure 21: Vorticity Distribution Normal to the Wall for TVD Scheme.

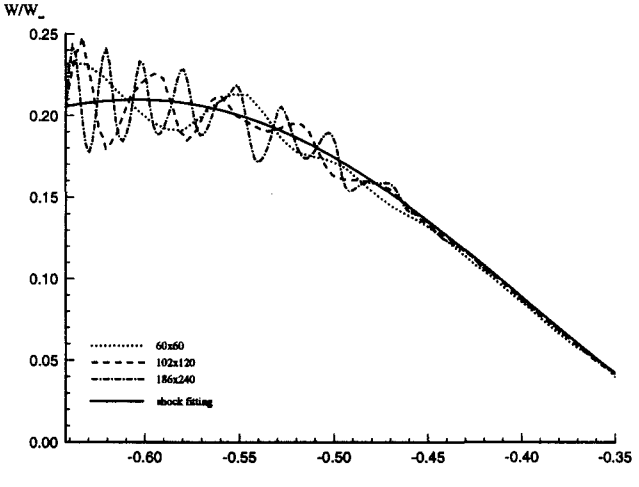

Figure 20: Vorticity Distribution Normal to the Wall for ENO Scheme.

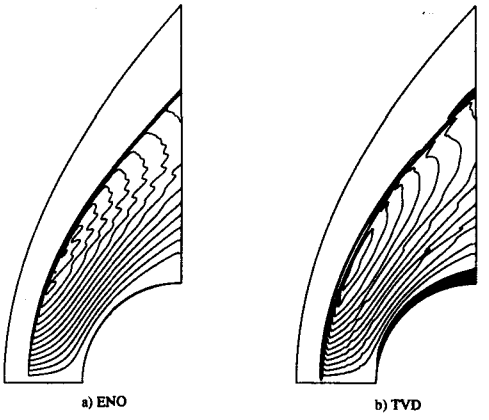

Figure 22: Vorticity Contours for ENO and TVD solutions Using Aligned Grid.

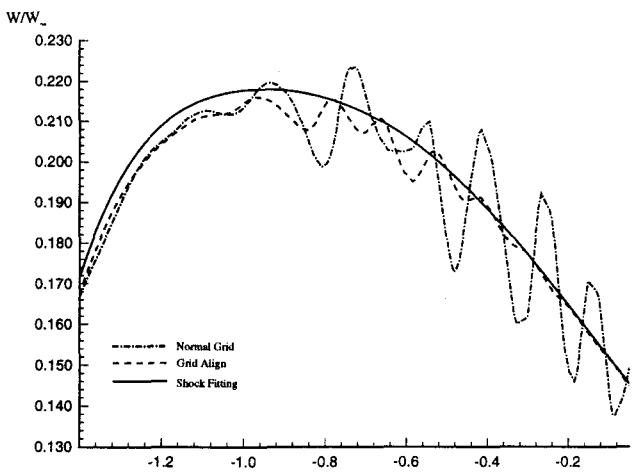

Figure 23: Vorticity Distribution Behind the Shock for ENO Scheme Using Aligned Grid.

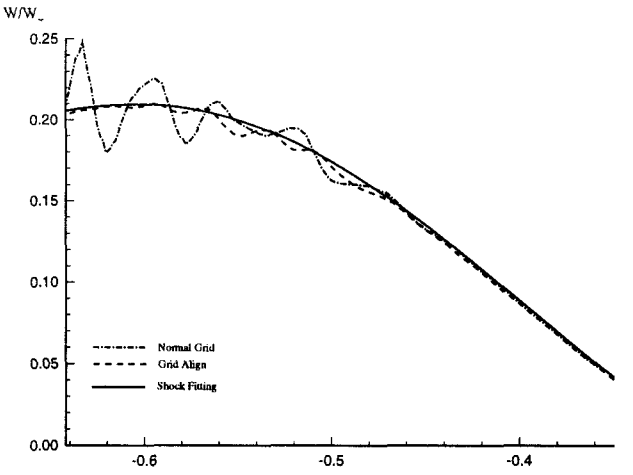

Figure 25: Vorticity Distribution Normal to the Wall for ENO Scheme Using Aligned Grid.

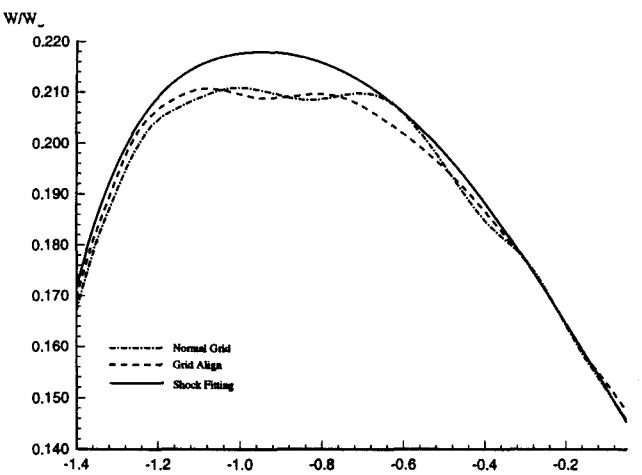

Figure 24: Vorticity Distribution Behind the Shock for TVD Scheme Using Aligned Grid.

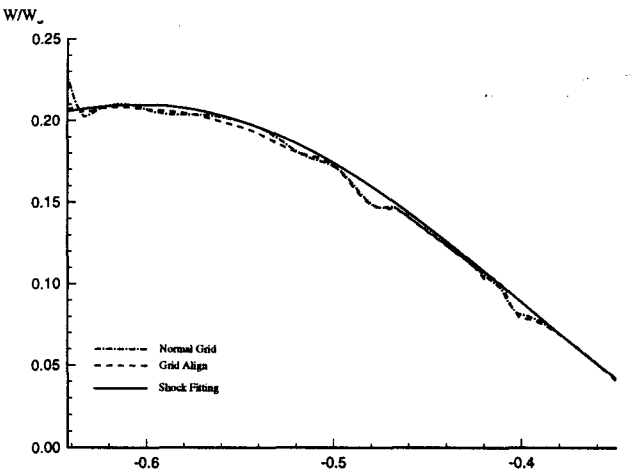

Figure 26: Vorticity Distribution Normal to the Wall for TVD Scheme Using Aligned Grid.